Record resistivity for in-situ grown horizontal carbon nanotubes interconnect

J. Dijon[1], R. Ramos[1], A. Fournier[1], H. Le Poche[1], H. Fournier[1], H. Okuno[2], J.P. Simonato[1]

Univ. Grenoble Alpes, F-38000 Grenoble, France
1 CEA, LITEN DTNM, 17 rue des Martyrs, 38054 Grenoble, France,
2 CEA, INAC SP2M, 17 rue des Martyrs, 38054 Grenoble, France,
Tel +33 4 38784313, fax +33 4 38785117 email: jean.dijon@cea.fr

ABSTRACT

An integration scheme for the in-situ growth and contacting of carbon nanotube (CNT) horizontal interconnects with densities of 1.10^{13} walls/cm^2, lengths up to 20 µm and diameters down to 50 nm is described. Doping of the CNT lines with iodine results in a record low resistivity of 450 µΩ.cm..

Keywords: carbon nanotube, interconnects, iodine doping

1 INTRODUCTION

Carbon in the form of nanotubes (CNTs) and graphene is the only known material that can replace copper in integrated circuits to carry the high current densities associated with advanced interconnects. Its implementation is however currently plagued by integration issues and poor electrical performances (both CNT resistivity and carbon/metal contact). The integration of CNTs in *vertical* interconnects (i.e. vias) was demonstrated and recently reviewed [1,2]. Even though high CNT area density can be achieved in vias [3], the gain from using CNTs instead of Cu is larger for the longer *horizontal* interconnects [2]. However, only few reports exist on the integration of CNTs in such interconnects. Here we demonstrate an integration scheme for the in-situ growth and contacting of horizontal CNT lines with lengths up to 20 µm and diameters down to 50 nm [4]. We also report for the first time the iodine doping of CNT interconnects resulting in the lowest resistivity reported for horizontal CNT interconnects with 450 µΩ.cm, i.e. comparable to the best CNT vias [1].

2 EXPERIMENT

2.1 CNT growth and process flow to make electrically contacted CNT lines

The unique process flow implemented is described in Fig. 1. The overall concept is to selectively grow dense bundles of CNTs (Fig. 2) in individual via structure on an Al bottom layer [3] and to subsequently flip the CNT bundles on the wafer surface using a specific technique used in MEMS fabrication [5]. After flipping of the bundles (Fig. 1), dense horizontal lines of triple wall CNTs (average diameter ~5 nm) are fabricated (Fig. 2). This modified CNT via integration scheme uses the same CNT growth mode as used for high density CNT mats. This mode used at 580°C works well on conductive substrates such as aluminium copper alloy layer (99.5% Al). To localise the tubes in the bottom part of the via hole, the iron catalyst layer deposited by e-beam evaporation is removed from the sample surface using ion beam etching at a 60° incidence from the normal. CNT growth was carried out with a mixture of C_2H_2, H_2 and He (ratio 1:5:5) at a pressure below 1 mbar. After alcohol flipping of the bundles with a

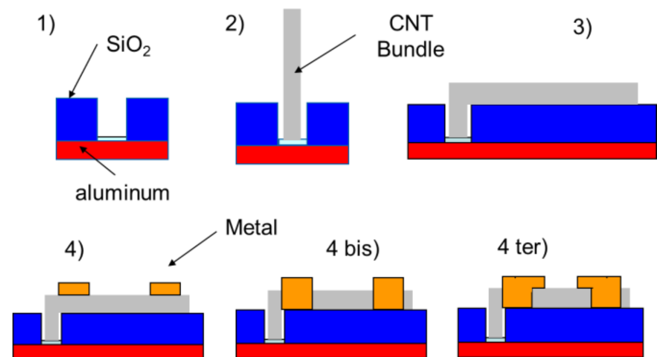

Fig 1: Process flow to make individual high density CNT line contacted with electrodes. 1) individual via structure used to growth CNT bundle 2) Long vertical CNT bundle grown in the via 3) Flipping of the bundle on the surface by alcohol dipping 4) line with side- bonded contact deposited on top 4bis) line with end-bonded contact between metal and CNT 4ter) line with all-around metal contact.

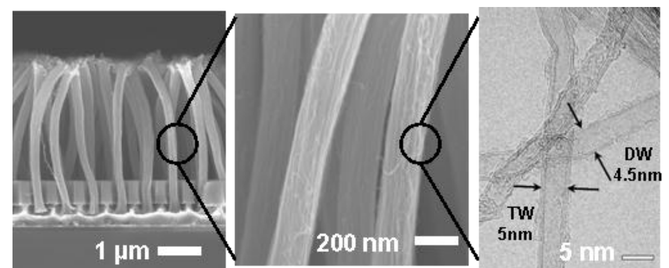

Fig 2: SEM view of ultra high density vertically aligned TW CNT ($3x10^{12}$ cm^{-2}) grown in via structure with Al

bottom line. The CNT density in the bundle after compaction is 9×10^{12} cm^{-2}

sliding tool, the contacts are deposited with three possible geometries (Fig. 1-4): side-bonded contact with the metal deposited on top of the bundle; end-bounded contact with the contact deposited after etching of the CNT bundle; or all-around contact wich mixes the two previous geometries and is favorable for low resistivity of long lines [6]. The device electrodes are circular, concentric, and centered on the individual via used as growth structure (Fig. 3). This geometry allows contacting of the bundles even if perfect bundle alignment is not obtained. Electrode gap ranging between 2 and 7 µm are implemented on the same chip.

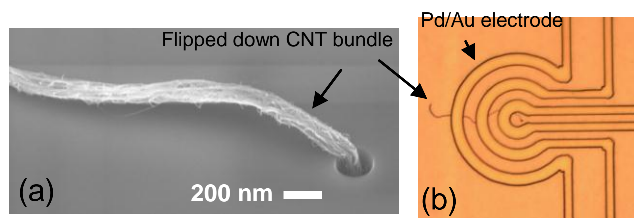

Fig 3: CNT line devices: a) CNT bundle emerging from a 200 nm diameter via flipped on the surface; b) electrode structure.

2.2 All Around contact structure

The details of the contact formation process was already published elsewhere [6]. Here we briefly highlight the formation of the original all-around contact geometry which was used in this work. A three layer stack composed of a LOR resine, a silica hard mask and a photoresist is deposited on the CNT bundle (Fig. 4). After photoresist patterning, the hard mask, LOR and CNTs are dry etched. An undercut in the LOR remaining on top of the CNTs is done by wet etching to allow simultaneous metal deposition on top and on the edge of the bundle.

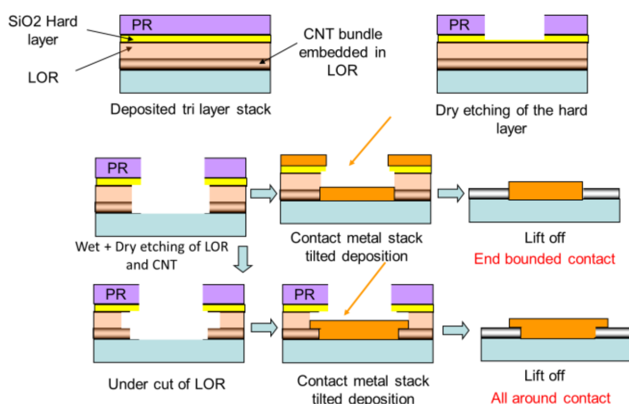

Fig 4: Process flows to make contact on flipped CNT bundles using a hard mask. In the middle, the process to make end-bonded contact with dry etching of the CNTs. At the bottom, the process to make All-Around contact with wet etching to undercut the LOR and expose the CNT side to metal.

The metal contact deposited at 20° incidence is a two layer system composed of 20 nm Pd and 200 nm gold (alternatively Ti/Au or Cr/Al [7]). Pd/Au was preferred here to avoid contact degradation by the iodine doping process. The electrode contact length on the CNT bundle is close to 500 nm (Fig. 5).

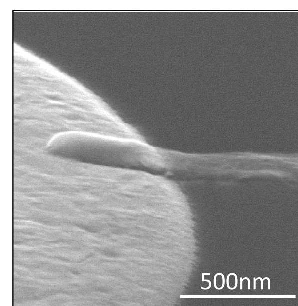

Fig 5: All-around contact of a CNT bundle with metal electrode.

2.3 Doping Procedure

After devices fabrication the samples are baked at 100°C during 6 hours in a sealed chamber loaded with solid iodine pellets. Vertically aligned carpet of CNTs grown in the same run were also doped and observed by HAADF/STEM with Z-contrast imaging (fig 6) . The tubes are clearly coated by heavy element after doping process. This indicates that the iodine is inserted between the tubes. The obtained doping is stable under ultra high vacuum conditions and annealing temperature up to 250°C.

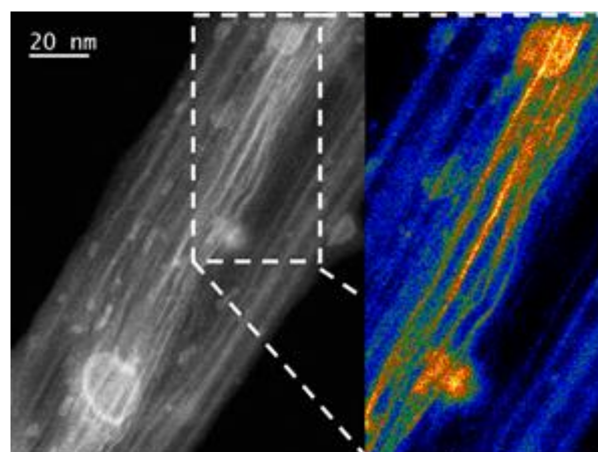

Fig 6: HAADF/STEM image of an I_2-doped CNT bundle showing interstitial iodine between the CNTs. On the right same image as left one coded with color intensity scale. The heavy iodine (yellow) is clearly on the walls not inside CNTs.

NSTI-Nanotech 2014, www.nsti.org, ISBN 978-1-4822-5830-1 Vol. 3, 2014

3 ELECTRICAL RESULTS

The same samples were measured before and after doping to correctly assess the role of dopant. The classical TLM method [8] is implemented by measuring device resistance R for different electrode gap G. The curve R(G) allows us to extract both the contact resistance and the line resistivity. Due to the bundle waviness between the electrodes the exact connection lengh is measured with SEM for each device. The electrical results before and after doping are presented in figure 7. Before doping the least square linear fit of the data gives a CNT line resistance per unit length of 2.3 kOhm/µm with a contact resistance of 2.1 kOhm. After doping, the contact resistance slightly increases to 2.6 kOhm while the line resistance considerably decreases to 590 Ohm/µm. The average CNT bundle diameter measured by SEM is 95 nm. This diameter leads to a record resistivity value of 450 µOhm.cm after doping for the CNT connection. The resistivity before doping is 1.5 mOhm.cm, consistent with our already published values [4]. The iodine doping thus leads to a conductivity improvement by a factor 3.8.

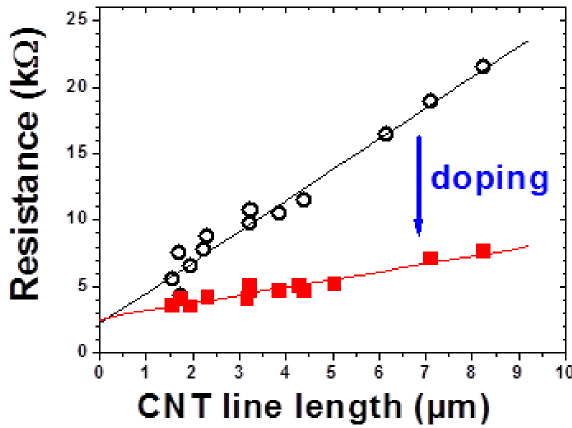

Fig 7: Resistance of 95 nm diameter horizontal CNT lines as a function of their lengths. Iodine doping of the interconnects reduces the resistivity by 380% and yields a record resistivity of 450 µΩ.cm.

4 DISCUSSION

Up to now, while promising predictions have been made on the potential of CNTs as a material to replace copper, experimentally reported CNT line resistivities surprisingly saturate at a lower limit around 1.5 mOhm.cm (Fig. 8). For short vias [9-12] previous extensive work shows that the main limitation is related to contact resistance of the tubes with the metal electrode. However for long lines [13-15] the intrinsic properties of the CNT material and the bundle structure are key aspects. Doping of CNT lines was already reported using platinum nanoparticles [14] with a conductivity improvement close to a factor of 3. The lowest ever measured conductivity on CNT bundles (i.e. 15 µOhm.cm) was achieved on macroscopic ultra dense bundle of CNTs doped with iodine for CNT cable applications [16]. On these cables the measured improvement in conductivity is a factor of 4, similar to our results. The differences in performance between CNT cables and integrated CNT lines (by a factor of 30) have yet to be understood and mastered in order to produce

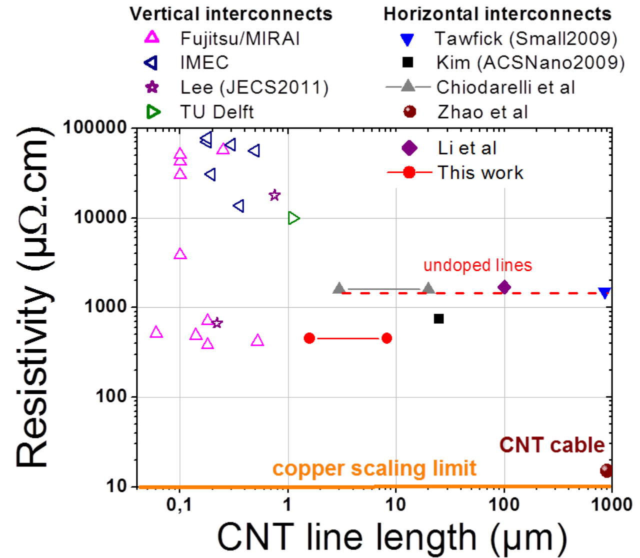

Fig 8: CNT interconnect resistivity versus length (closed and open symbols for horizontal and vertical interconnects, respectively). The resistivity target for VLSI is below 10 µOhm.cm. All the published values concerning undoped lines are close to 1.5 mOhm.cm

interesting enough results and to promote CNT interconnects from brillant future to reality. The performances improvement likely relies on the density of CNTs, on the intrinsic tube quality and on the number of properly contacted tubes in the bundle (structure of the metal contact [7]). In any case we believe ultimate performances will undoubtedly need CNT doping and our preliminary results show that it can be successfully achieved with iodine in the context of small diameter interconnects.

ACKNOWLEDGMENTS

The authors would like to acknowledge Intel Corporation for financial support of this work and in particular Intel's B Capraro and J. McKenna for providing us the via structure.

REFERENCES

[1] Y. Awano *et al*, Proc. IEEE **98**, 2015 (2010)

[2] J. Robertson *et al,* Jpn. J. Appl. Phys. **51**, 01AH01 (2012)
[3] J. Dijon *et al*, IEDM 2010 IEEE p. 33.4 (2010)
[4] N. Chiodarelli, A. Fournier, H. Okuno, J.Dijon, Carbon **60,** 139 (2013)
[5] Y. Hayamizu *et al*, Nature Nanotech **3**, 289 (2008)
[6] N. Chiodarelli, A. Fournier, and J. Dijon Applied Physics Letters **103**, 053115 (2013)
[7] J. Dijon et al, MRS proc vol 1559 (2013) DOI :10.1557/opl.2013.869
[8] G.K Reeves, H.B. Harisson IEEE Electron devices Lett **3** (5), 111-3 (1982)
[9] Kawabata et al. IEEE, IITC , art. no. 4546977, pp. 237-239 (2008)
[10] M.H. van der Veen et al./Microelectronic Engineering 106 (2013)106–111
[11] S.Lee et al. JECS 158 (11) K193-K196 (2011)
[12] S. Vollebregt et al., IEEE IITC conf. proc. (2012) 1–3
[13] S. Tawfick, K. O'Brien, A. J. Hart Small **5**, No. 21, 2467–2473 (2009)
[14] Y.L. Kim, Bo Li, X. An et al ACS nano **3** n° 9 2818–2826 (2009)
[15] H.Li, W.liu AM Cassell F. Kreupl, K. Banerjee IEEE trans. on electron device **60** n°9 2862 (2013)
[16] Yao Zhao et al SCIENTIFIC REPORTS | 1 : 83 | DOI: 10.1038/srep00083